

RSC Advances

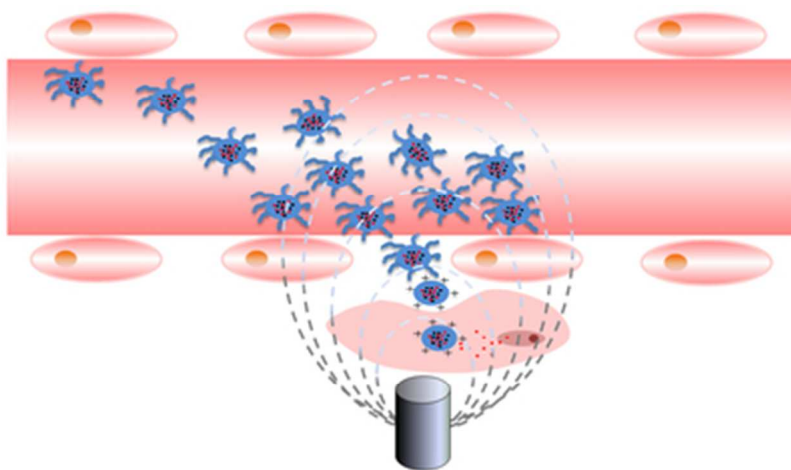


This is an *Accepted Manuscript*, which has been through the Royal Society of Chemistry peer review process and has been accepted for publication.

Accepted Manuscripts are published online shortly after acceptance, before technical editing, formatting and proof reading. Using this free service, authors can make their results available to the community, in citable form, before we publish the edited article. This *Accepted Manuscript* will be replaced by the edited, formatted and paginated article as soon as this is available.

You can find more information about *Accepted Manuscripts* in the [Information for Authors](#).

Please note that technical editing may introduce minor changes to the text and/or graphics, which may alter content. The journal's standard [Terms & Conditions](#) and the [Ethical guidelines](#) still apply. In no event shall the Royal Society of Chemistry be held responsible for any errors or omissions in this *Accepted Manuscript* or any consequences arising from the use of any information it contains.



Graphical Abstract. Magnetic- and pH- dually sensitive drug delivery system
39x19mm (300 x 300 DPI)

Cite this: DOI: 10.1039/c0xx00000x

www.rsc.org/xxxxxx

ARTICLE TYPE

Magnetic and pH Sensitive Drug Delivery System through NCA Chemistry for Tumor Targeting

Jingjing Wang^a, Chu Gong^a, Yinong Wang^a, Guolin Wu^{a,b,*}*Received (in XXX, XXX) Xth XXXXXXXXXX 20XX, Accepted Xth XXXXXXXXXX 20XX*

DOI: 10.1039/b000000x

For the purpose of tumor-specific drug delivery applications, a magnetic and pH dually responsive nano-carrier with a multilayer core-shell architecture was prepared from amine-functionalized Fe₃O₄@SiO₂ through the surface-initiated ring opening polymerization of benzyl-L-aspartate N-carboxyanhydride, and then coated with α -methoxy poly(ethylene glycol) (mPEG) via a pH-sensitive benzoic-imine bond. In order to control the layer thickness of poly(benzyl-L-aspartate) (PBLA), a surface passivation agent was applied to modulate the amino density of the functionalized Fe₃O₄@SiO₂ initiator. In this system, the Fe₃O₄@SiO₂ nanoparticles function as a superparamagnetic core used to target the drug loaded nanocarriers to pathological site. Meanwhile, the mPEG and PBLA segments serve as a pH-sheddable hydrophilic corona and a hydrophobic middle layer used to load the drug via hydrophobic interactions, respectively. The obtained materials were characterized by FT-IR, ¹H NMR, DLS, zeta-potential, TEM, TGA and hysteresis loop analysis. Furthermore, the loading and release behavior of doxorubicin on the nanocarrier was investigated and it was shown that the drug loaded nanoparticle was relatively stable under physiological conditions and quickly released in response to acidity due to the shedding of mPEG shells through the pH-cleavage of intermediate benzoic-imine bonds. This pH and magnetic responsive nanoparticle has appeared highly promising for the targeted intracellular delivery of hydrophobic chemotherapeutics in cancer therapy.

Introduction

Magnetism is an advantageous physical stimulus that can be utilized to direct the drug-loaded nanocarriers to the specific target pathological sites.^{1,2} The concept of the magnetic assisted drug delivery system was first proposed by Widder et al. in 1978.³ After being coated with polymeric materials, magnetic particles (MPs) would be more suitable as drug carriers, due to their high stability, superparamagnetism and high biocompatibility. A combination of magnetic nanoparticles with multifunctional drug delivery platforms is crucial for the realization of precise and controlled release of chemotherapeutics.

Polypeptides are provided with unique structures, biocompatibility, biodegradability, and various side groups for further functionalization. They have been extensively studied as carriers for drug delivery. Recently, a magnetic responsive nanocarrier with multilayer core-shell architecture was developed in our group by grafted α -methoxy poly(ethylene glycol)-poly(L-asparagine) onto the SiO₂-coated Fe₃O₄ nanoparticles via a condensation reaction through amide linkages.⁴ However, it was hard to control the polypeptide grafting density and the particles were not highly uniform in this system. Xu and co-workers have

designed a polypeptide-coated Fe₃O₄ nanoparticle formed by N-carboxyl anhydride ring-opening polymerization (NCA-ROP) initialized by amino functionalized MPs.⁵ As the steric hindrance, it was also hard to control the thickness of the polypeptide shell in this system. In this study, a surface passivation agent was employed to take up a proportion of free amine sites, which could reduce the steric hindrance between growing polymeric chains during NCA-ROP and was beneficial to control the shell thickness.

For drug delivery nanocarriers, surface modification of nanoparticles (NPs) with polyethylene glycol (PEG), the so-called PEGylation, is the most commonly used approach for reducing the premature clearance of NPs by reticuloendothelial system and extending the blood lifetime of injected NPs.^{6,7} However, after locating at the target, nanocarriers should be able to deliver their payloads in an efficient way. It was reported that the PEG surfaces would limit interactions between the nanocarriers and target tissues and sequentially diminish cellular uptake of the loaded contents.^{8,9} PEG-sheddable nanoparticles, which are able to shed their outer layers when target the pathological site, may facilitate the drug release as well as the interaction with target cells. Nanoparticles with pH-sheddable

PEG layers conjugated via an acid cleavable linkage, such as hydrazone, thiopropionate, acetal, or orthoester have been reported to enhance the intracellular drug delivery.¹⁰⁻²² Yang and his co-worker reported an amphiphilic copolymer prepared by conjugating PEG and a hydrophobic block through benzoic-imine bonds. The benzoic-imine linker is more stable than imine bond at neutral and basic pH due to its extended π - π conjugation, and is cleavable following a decrease in pH.^{23,24}

In this paper, a magnetic and pH dual-responsive core-shell-corona structure drug delivery nanocarrier was prepared by using the SiO₂-coated Fe₃O₄ nanoparticle as the core, poly(benzyl-L-aspartate) (PBLA) as the shell, and the pH-sheddable α -methoxy poly(ethylene glycol) (mPEG) as the corona. In which, highly content of peptide grafting was obtained by partial passivation of the initiating core surface with a certain percentage of methyltrimethoxysilane to prevent crowding of the PBLA chains that grew via the NCA-ROP of benzyl L-aspartate NCA from amino-functionalized Fe₃O₄@SiO₂ nanoparticles. The mPEG chains were subsequently connected to the surface of particles via benzoic-imine bonds. In addition, the hydrophobic anticancer drug doxorubicin (DOX) was loaded into the magnetic composite nanoparticles, and their drug release performance was investigated under physiological conditions and acidic condition. In this system, the cleavage of the benzoic-imine bonds and shedding of the PEG layer at acidic conditions are expected to facilitate the drug release.

Experimental details

Materials

Ferric trichloride hexahydrate (FeCl₃·6H₂O), ferric dichloride tetrahydrate (FeCl₂·4H₂O) and 4-carboxybenzaldehyde were purchased from Aladdin Reagent Company. The L-aspartic acid was supplied by United Star Biological Co. Tetraethoxysilane (TEOS), methyltrimethoxysilane (MTMS), 3-(aminopropyl)triethoxysilane (APTS) and mPEG (Mn=1900) were obtained from Alfa Aesar. N,N-dimethylformamide (DMF) and tetrahydrofuran (THF) were distilled under reduced pressure before use. DOX hydrochloride (DOX·HCl) was supplied by Beijing Huafeng United Technology CO. Other chemicals were all of analytical reagent grade and used as received.

Measurements

¹H NMR spectrum was recorded on a Varian UNITY-plus 400 NMR spectrometer using CDCl₃ as solvent. Tetramethylsilane was used as the internal standard. Fourier transform infrared spectra (FT-IR) were measured using a Bio-Rad FTS6000 spectrophotometer with a resolution of 4 cm⁻¹ at room temperature. Magnetic nanoparticles were prepared by well milling in KBr powder and compressing the mixtures to form a plate. The morphology and size of the magnetic nanoparticles were observed by transmission electron microscope (TEM). The digital images were recorded on a JEM2100EX microscope. To prepare the samples, a small drop of magnetic nanoparticle dispersion was drop-cast onto a carbon-coated copper grid. The particle size and zeta potential of the magnetic nanoparticle were determined with a Zetasizer nano ZS90 (Malvern Instruments, U.K.) with an argon laser beam at a wavelength of 670 nm at 25 °C and 90° of scattering angle. The magnetic properties were

measured by a vibrating sample magnetometer (LDJ-9600VSM). Thermogravimetric analyzer (TGA) was used to investigate the polymers' stability in a nitrogen atmosphere at a heating rate of 10 °C·min⁻¹.

Synthesis of magnetic nanoparticles (Fe₃O₄)

Fe₃O₄ magnetic nanoparticles were synthesized by chemical co-precipitation. In general, FeCl₃·6H₂O (4.70 g, 17.4 mmol) and FeCl₂·4H₂O (1.72 g, 8.6 mmol) dissolved in deoxygenated distilled water (80 mL) was stirred with ammonia (10 mL) at 80 °C for 30 min. The product was washed with deoxygenated distilled water and anhydrous ethanol by magnetic separation before dried under vacuum. To obtain the well-dispersed Fe₃O₄ nanoparticles, the prepared Fe₃O₄ nanoparticles were added into 0.1 M sodium citric (10 mL) with ultrasonic for 30 min, and then the reaction was kept for 12 h at room temperature. The obtained citric modified nanoparticles (Fe-Cit) were isolated using magnetic separation and dried under vacuum.

Synthesis of silica coated magnetic nanoparticles (Fe₃O₄-SiO₂)

First, the synthesized citric modified Fe₃O₄ nanoparticles (Fe-Cit, 60 mg) were dispersed in H₂O/ethanol (1:4) with ammonia (7 mL) to adjust the solution pH, and then TEOS (1 mL) was added. The mixture was stirred at room temperature and N₂ atmosphere for 5 h. Next, the product was washed with deoxygenated distilled water and anhydrous ethanol by magnetic separation. Finally, silica coated Fe₃O₄ magnetic nanoparticles were obtained by drying in vacuum overnight.

Surface modification of Fe₃O₄-SiO₂

APTS (60 μ L) or a mixture of APTS and MTMS (25% APTS and 75% MTMS) was added into the ethanol suspension of Fe₃O₄-SiO₂ (100 mg), and stirred at 70 °C for 12 h before the black solid product was extracted and washed by H₂O/ethanol (80/20) to obtain amino modified Fe₃O₄-SiO₂ nanoparticles FeSi100-NH₂ or FeSi25-NH₂.

Synthesis of peptide brush-magnetic nanoparticles (FeSi25@PBLA and FeSi100@PBLA)

Benzyl-L-aspartate NCA (BLA-NCA) was synthesized according to our previously reported work.⁴ FeSi25-NH₂ or FeSi100-NH₂ was used as a macro-initiator for ring opening polymerization of BLA-NCA. In general, FeSi25-NH₂ (50 mg) (or FeSi100-NH₂) and BLA-NCA (5.6 g, 22.5 mmol) were dissolved in anhydride DMF (50 mL) and stirred for 3 days at 35 °C under N₂ atmosphere. Ethyl ether was added to form a brown precipitation. FeSi25@PBLA (or FeSi100@PBLA) was removed by magnetic separation and rinsed thoroughly with DMF and anhydrous ethanol before dried under vacuum.

Synthesis of pH and magnetic sensitive nanocomposites (FeSi25@PBLA@mPEG and FeSi100@PBLA@mPEG)

Firstly, mPEG-CHO was synthesized. In brief, mPEG (8.0 g, 4 mmol), 4-Carboxybenzaldehyde (6.0 g, 40 mmol, 10 equiv), DCC (8.2 g, 40 mmol) and DMAP (1.2 g, 10 mmol) were added in dichloromethane (DCM) (150 mL) and stirred for 24 h at room temperature. Then the solution was filtered. The filtrate was concentrated and isopropanol (180 mL) was added in to form a white precipitation. After 5 h, the resulting product mPEG-CHO

was collected by filtration and washed with isopropanol and diethyl ether.

Then, FeSi25@PBLA (or FeSi100@PBLA) (300 mg) and mPEG-CHO (600 mg) were dispersed in DMSO (15 mL), and stirred at 40 °C for 24 h. Finally, the reaction mixture was dialyzed against 0.01 M PBS (pH 7.4) for two days. The product (FeSi25@PBLA@mPEG or FeSi100@PBLA@mPEG) was freeze-dried.

Preparation of DOX-Loaded nanocomposites

DOX-loaded nanocomposites were prepared as follows: briefly, FeSi25@PBLA@mPEG (30 mg) (or FeSi100@PBLA@mPEG) and DOX·HCl (6 mg) were dispersed in DMSO (10 mL) with triethylamine (10 μL) to neutralize the HCl. The mixture was stirred overnight and then dialyzed against 0.01 M PBS (pH 7.4) for two days. DOX-loaded nanocomposites were lyophilized to give a deep red powder. The dried samples were weighed and dissolved in DMSO. After the insoluble Fe₃O₄-SiO₂ particles were removed from the solution by magnetic field-guided accumulation, the absorbance of DOX at 485 nm was measured to determine drug content in the solution. The drug loading efficiency (LE%) was calculated by the following equations:

$$LE\% = \frac{W_e}{P_o} \times 100$$

, where W_e and P_o are the weight of capsulated drug and magnetic nanocomposites with drug, respectively.

In vitro drug release assay

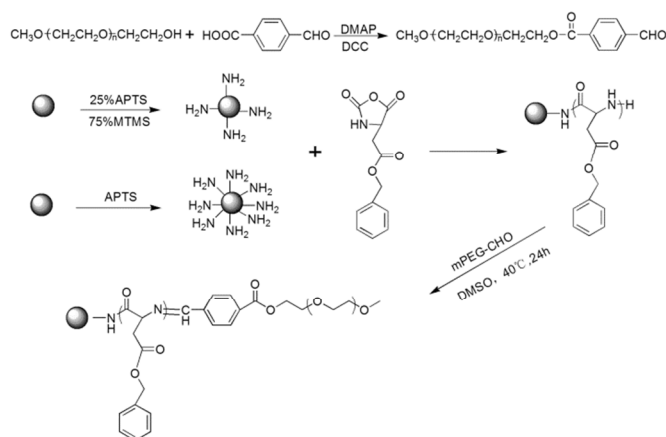
The release of DOX from the magnetic nanocomposites was evaluated in buffer solutions of pH 7.4 (0.01 M PBS) and 4.0 (0.01 M acetate buffer) by dialysis method, which were immersed into 10 mL buffer solution of the same pH value. The vials were placed in a shaking bed at a rate of 120 rpm at 37 °C. At selected time intervals, 3 mL of outside release media was taken out for measurement, and replaced with an equal volume of fresh buffer solution. The absorbance of DOX at 485 nm was measured to determine drug content in the solution. The cumulative released DOX was used to indicate the percentage of the total DOX available with a function of time.

Cytotoxicity test

The cytotoxicity of FeSi25@PBLA@mPEG was assessed in NIH/3T3 (mouse fibroblast cell line) cells by MTT assay. NIH/3T3 cells were seeded in a 96-well microtiter plates with 1×10^4 cells per well in DMEM complete medium and incubated at 37 °C in 5% CO₂ for 24 h. Then the polymer concentrations ranging from 0 to 200 μg·ml⁻¹ (0, 10, 50, 100 and 200 μg·ml⁻¹) were prepared and added into the medium for 48 h. After that, the solutions were aspirated, and replaced with MTT dye (100 μL, 0.5 mg·ml⁻¹ in PBS). After 4 h of further incubation, the MTT solutions were removed and dimethyl sulfoxide (150 μL) was added to dissolve the formazan crystals. Finally, the absorbance at 570 nm was read on a microplate reader, and the percentage of cell viability was measured relative to the negative control (media alone). Six replicates were counted for each sample. The mean values were used as the final data.

MTT assay was also used to evaluate cytotoxicity of the prepared DOX loaded nanoparticle. The process was the same as

above. NIH-3T3, MCF7 (human breast cancer cell line), and Hela (human cervical cancer cells) were used to compare the cytotoxicity of FeSi25@PBLA@mPEG@DOX nanocomposites to normal cells and tumor cells. The percentage of cell viability was measured relative to the negative control (media alone) and the positive control (triton X-100).



Scheme 1. Synthesis of pH and magnetic sensitive nanoparticles FeSi25/100@PBLA@mPEG.

Results and Discussion

Synthesis and Characterization of Block Copolymers

Particle production began with the creation of a silica coated magnetic core, which was functionalized with reactive amino groups used to initiate the ring-opening polymerization of NCA monomers. Firstly, the Fe₃O₄ nanoparticles were prepared by co-operation of ferrous and ferric salts with concentrated ammonia as a catalyst.²⁵ Magnetic nanoparticles are very sensitive to oxygen, and in the presence of air some may undergo oxidation to Fe(OH)₃ or γ-Fe₂O₃. Sodium citrate was used to modify on the surface after Fe₃O₄ nanoparticles were synthesized. After that, amorphous silica was used to coat on magnetic nanoparticles to obtain stable nanoparticles. Dr. Russo reported that partial passivation of the initiating core surface with a certain percentage of nonreactive groups can prevent crowding of the polypeptides that grow from the amino functionalized groups.^{26, 27} In this system, APTS was used to supply the amine functionality. MTMS is a silane lacking an amino functional group. It was used as a surface passivation agent in this work. The successful functionalization of the Fe₃O₄ surface with APTS and MTMS was confirmed by zeta-potential measurements (Table 1). The zeta-potential of Fe₃O₄-SiO₂, FeSi25-NH₂ and FeSi100-NH₂ are found to be -40 mV, +7 mV and +25 mV, respectively, which indicate the surface functional groups change from hydroxyl groups to amino groups. The higher zeta potential indicates more amino groups on the particle surface. The zeta potential results confirmed that adding MTMS is an effective approach to control the surface amino-functionalization and accordingly reduce the surface initiator density. Besides, the average particle diameters for Fe₃O₄-SiO₂, FeSi25-NH₂ and FeSi100-NH₂ were 115, 178 and 187 nm, respectively.

After the surface amino-functionalization, PBLA and PEG-CHO were successively conjugated to the magnetic nanoparticles via NCA-chemistry and pH-sensitive benzoic-imine bonds as

shown in Scheme 1. MPEG-CHO was obtained by the reaction of mPEG with 4-carboxybenzaldehyde. The structure of mPEG-CHO was determined using ^1H NMR analysis (Fig. 1), the conversion ratio of the aldehyde group was 98% determined by comparing the proton peak of -CHO (*f*) with the methoxy peak of mPEG-CHO (*a*).

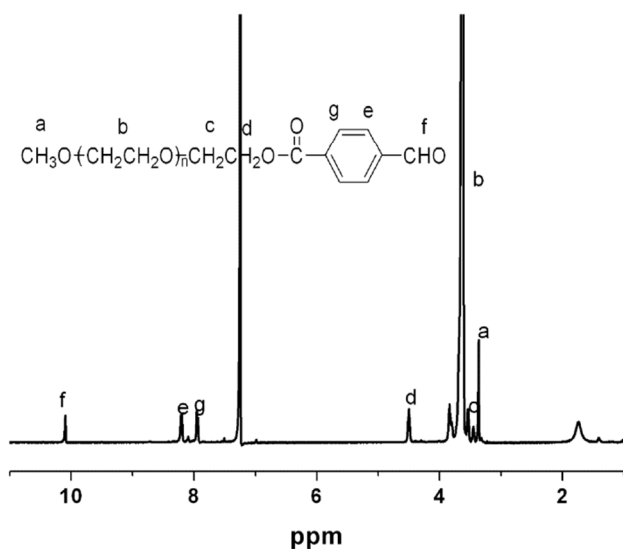


Figure 1 ^1H NMR spectrum of mPEG-CHO in CHCl_3

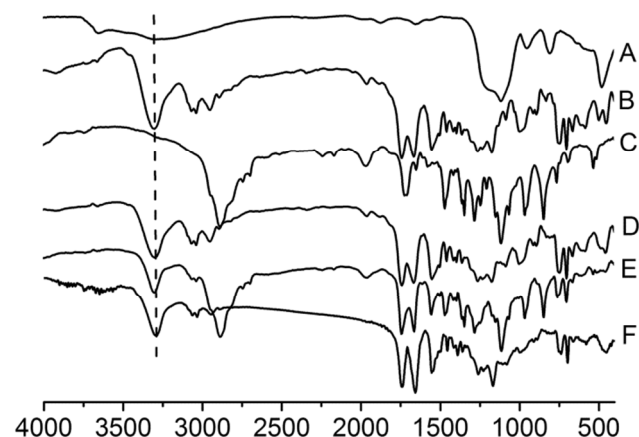


Figure 2 FT-IR spectra of FeSi25-NH₂ (A), PBLA (B), PEG (C), FeSi25@PBLA (D), FeSi25@PBLA@mPEG (E) and FeSi25@PBLA@mPEG-shedded (F)

The FT-IR spectra of FeSi25-NH₂, PBLA, mPEG, FeSi25@PBLA and FeSi25@PBLA@mPEG were shown in Fig. 2. In Fig. 2A, the stretching vibration of the Fe-O appeared at 592 cm^{-1} . The peaks at 1188 and 801 cm^{-1} were attributed to the asymmetric and symmetric stretching of Si-O-Si, respectively. Besides, the characteristic peak of the amino groups was appeared at 3296 cm^{-1} . The peak at 1740 cm^{-1} corresponded to the absorption peak of carbonyl group in -COOCH₂Ph. The peaks at 1660 cm^{-1} and 1550 cm^{-1} were attributed to the N-C stretching vibration of amide linkage. These proved that polyaspartate was grafted on the particles successfully. New peaks at 1100 and 2880 cm^{-1} emerged in Fig. 2E corresponded to the vibration of C-O and the symmetric vibration of -CH₂- in mPEG segments, respectively. In order to support the hypothesis of pH-responsive mPEG shedding, the FT-IR spectrum of FeSi25@PBLA@mPEG

washed at pH 5.0 was shown in Fig. 2F. The peaks at 1100 and 2880 cm^{-1} disappeared in Fig. 2F due to the shedding of mPEG during the cleavage of benzoic-imine bonds.

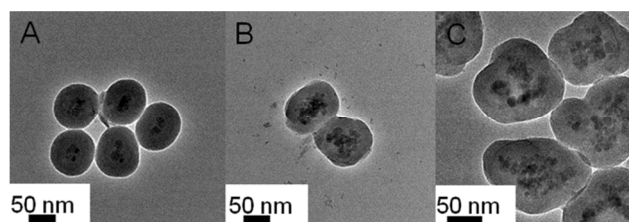


Figure 3. TEM of FeSi25-NH₂ (A), FeSi25@PBLA (B), and FeSi25@PBLA@mPEG (C)

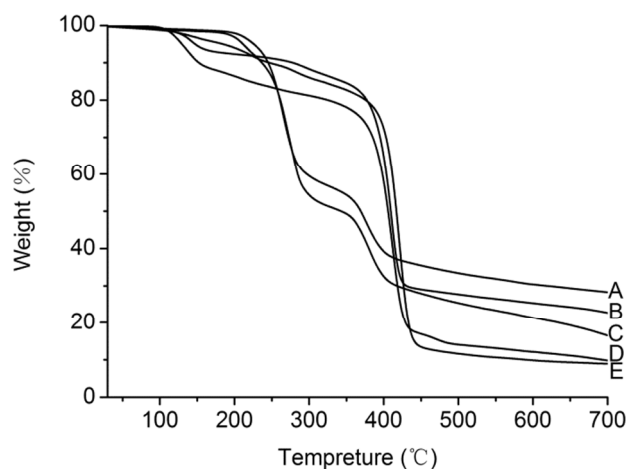


Figure 4. TGA curves of FeSi100@PBLA (A), FeSi100@PBLA@mPEG (B), FeSi25@PBLA (C), FeSi25@PBLA@mPEG (D) and FeSi25@PBLA@mPEG@DOX (E)

The TEM images of the magnetic nanoparticles are presented in Fig. 3. After silica coating, no aggregation was observed. From Fig. 3B to Fig. 3C, particle size increased from 80 nm to around 150 nm with a hazy layer around the solid core.

TGA was carried out to determine the graft density of PBLA and mPEG coated on Fe₃O₄. Fig. 4 shows the TGA curves of FeSi100@PBLA, FeSi100@PBLA@mPEG, FeSi25@PBLA, FeSi25@PBLA@mPEG and FeSi25@PBLA@mPEG@DOX. The derivatives of the weight loss as a function of temperature were shown in Fig. S1†. Based on the TGA results, it could be defined that the ratios of PBLA and mPEG in FeSi100@PBLA@mPEG were 63.0% and 5.5%, respectively. While the ratios of PBLA and mPEG in FeSi25@PBLA@mPEG were 70.9% and 6.7%, respectively. The TGA results indicated that appropriate passivation of the initiating surface can effectively prevent the crowding of the polymeric chain that grow from the surface of the particles and provide a good uniformity at high degrees of polymerization, and will not decrease the grafting ratio of mPEG in this system.

When the mixture of DOX and polymer was extensively dialyzed against PBS (pH 7.4), the key factor for DOX loading into nanoparticles is the hydrophobic interaction between the benzyl group and DOX molecules. In addition, the π - π stacking between benzyl and DOX may also contribute to the loading efficiency. TGA (Fig. S1†) results showed that the LE% for FeSi25@PBLA@mPEG was 10.7%. It was consistent with the result determined by UV-vis (10.1%). As the iron and silica core

took most of the weight, the LE% of this complex was relatively low comparing with pure polymeric drug carrier systems.

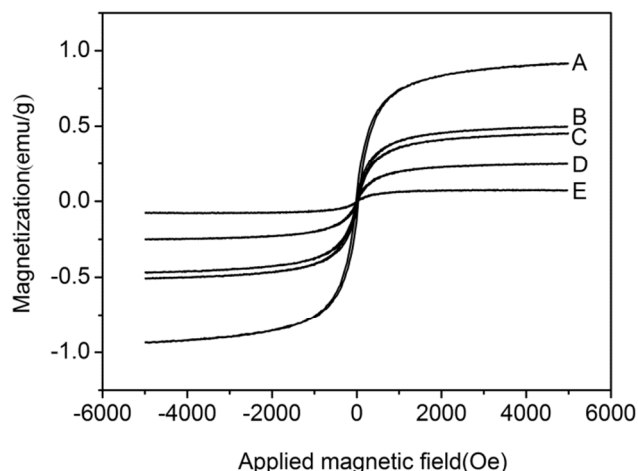


Figure 5. Hysteresis loops of FeSi100@PBLA (A), FeSi100@PBLA@mPEG (B), FeSi25@PBLA (C), FeSi25@PBLA@mPEG (D) and FeSi25@PBLA@mPEG@DOX (E)

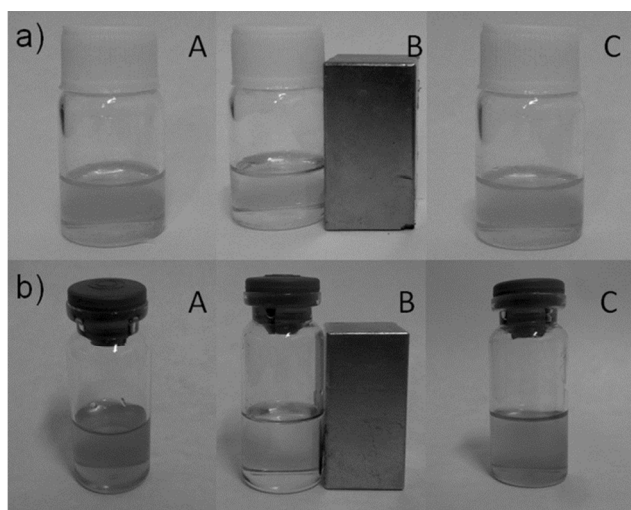


Figure 6. Photographs of the (a) FeSi25@PBLA@mPEG@DOX and (b) FeSi100@PBLA@mPEG@DOX dispersed in aqueous solution (A) static condition, (B) after the application of a localized magnetic field and (C) re-dispersion after removing the magnetic field.

The hysteresis loops of FeSi100@PBLA, FeSi100@PBLA@mPEG, FeSi25@PBLA, FeSi25@PBLA@mPEG and FeSi25@PBLA@mPEG@DOX are shown in Fig. 5. The results demonstrated that these nanoparticles manifest superparamagnetic behavior with almost immeasurable coercivity and remanence. The magnetic saturation values of FeSi100@PBLA, FeSi100@PBLA@mPEG, FeSi25@PBLA, FeSi25@PBLA@mPEG and FeSi25@PBLA@mPEG@DOX were 0.89, 0.50, 0.44, 0.25 and 0.07 emu/g, respectively. The saturation magnetization value is related to the amount of iron oxide nanoparticles; as nanoparticle coating is increased, the amount of iron oxide in the magnetic composite nanoparticles is reduced. Therefore, the decrease of the saturation magnetization value is attributed to the existence of coated polymers and encapsulated DOX on the surface of Fe₃O₄ nanoparticles. The

saturation magnetizations of the magnetic particles are in agreement with the results obtained from the TGA measurements.

Although the saturation magnetization values were relatively low, FeSi25@PBLA@mPEG@DOX and FeSi100@PBLA@mPEG@DOX composite nanoparticles also showed quickly responsiveness to an external magnet (Fig. 6). For the dispersed solutions, the nanoparticles could be swiftly gathered on the surface of the reagent bottle when a magnet was placed at the side, the homogeneous deep red dispersion (Fig. 6A, the UV-absorbance of FeSi25@PBLA@mPEG@DOX nanoparticles was shown in Fig. S2†) became clear (Fig. 6B) in 1 min. Removing the magnet, the accumulated nanoparticles were re-dispersed (Fig. 6C). These results suggested that the magnetic hybrid encapsulation could be easily manipulated by applying an external magnet field. The well effectiveness and reversible response of the nanoparticles in a magnetic field are very important for their drug delivery applications.

Table 1. Diameter and zeta-potential of magnetic nanoparticles.

Sample	Size (d-nm)	PDI	Zeta potential (mV)
Fe ₃ O ₄ -SiO ₂	115	0.048	-40
FeSi25-NH ₂	178	0.054	+7
FeSi100-NH ₂	187	0.043	+25
FeSi25@PBLA	230	0.157	+2
FeSi100@PBLA	248	0.183	+7
FeSi25@PBLA@mPEG	245	0.265	-3
FeSi100@PBLA@mPEG	257	0.237	-4
FeSi25@PBLA ^a	223	0.324	+2

^a FeSi25@PBLA@mPEG nanoparticles after mPEG layer shedding at acidic condition.

The diameters and zeta-potentials of the nanoparticles were also measured to monitor the entire preparation process and are listed in Table 1. After PBLA grafted on the macroinitiator, the zeta potential of FeSi25-NH₂ and FeSi100-NH₂ decreased from +7 and +25 mV to +2 and +7 mV, respectively. Meanwhile, the particle size increased from 178 and 187 nm to 230 and 248 nm, respectively. After the mPEG chains were decorated onto the surface of particles via benzoic-imine bonds, the size of FeSi25@PBLA@mPEG and FeSi100@PBLA@mPEG particles increased to 245 and 257 nm, respectively, while the zeta potential of FeSi25@PBLA@mPEG and FeSi100@PBLA@mPEG particles decreased to -3 and -4 mV, respectively. It should be noted that the sizes of the FeSi25@PBLA@mPEG or FeSi100@PBLA@mPEG nanoparticles observed by TEM were much smaller than those determined by DLS. This was attributed to the fact that the DLS measurements determined hydrodynamic diameter and were carried out in aqueous, when the mPEG layer is fully hydrated.

However, drying of the sample for TEM measurement and the ultrahigh vacuum conditions required for TEM studies leads to extensive dehydration of the complex, leading to a marked decrease in the observed particle size.

Under acidic conditions, the mPEG layer was shed, the size of FeSi25@PBLA@mPEG nanoparticles decreased to 223 nm, when its zeta potential increased to +2 mV. This is expected, because the hydrolysis of imine bonds generates amino groups, which would affect the charge properties of the system.

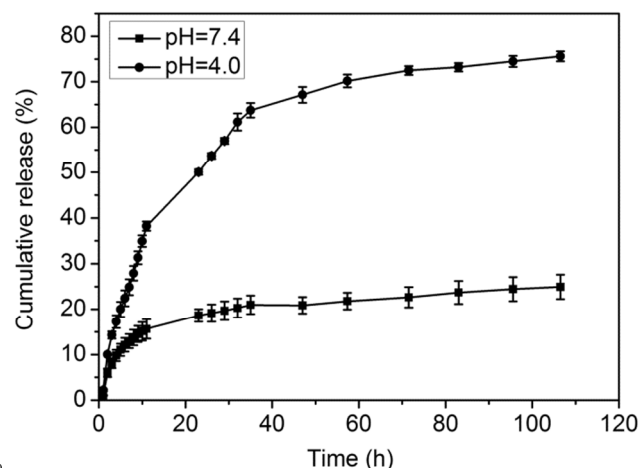


Figure 7. The pH-dependent DOX release profiles of FeSi25@PBLA@mPEG@DOX at pH 4.0 and 7.4 at 37 °C.

The *in vitro* release of DOX from FeSi25@PBLA@mPEG@DOX complex nanoparticles was carried out at pH 4.0 and 7.4 and showed well-defined pH-dependent drug release behaviour (Fig. 7). At pH 7.4, after the initial burst release of about 15%, the drug release rate was relatively slow and was further reduced after 10 h. The cumulated release amount was less than 20% after 50 h. However, the release of DOX loaded nanoparticles at pH 4.0 was much faster and more complete. After 50 h, about 65% of the drug was released at pH 4.0, and the drug release was still continuing. This pH-responsive drug release behaviour is due to the pH-sensitive cleavage of the benzoic-imine bonds.

Korsmeyer-Peppas equation was used to study the mechanism of DOX release:

$$Q_t/Q_e = k_{kp} t^n$$

, where Q_t/Q_e is the drug fraction released at time t , and k_{kp} and n are the constant corresponding to the structural and the kinetic exponent which is indicative of the mechanism of drug release, respectively. According to the equation for the initial several hours of drug release under various conditions, the correlation coefficient (R^2) is higher than 0.99, while the kinetic exponent at pH 7.4 and 4.0 are 0.45 and 0.83, respectively. This indicates that the kinetics of DOX release is typical Fickian diffusion at pH 7.4. While at pH 4.0, the release of DOX is random diffusion controlling kinetic, which is combined with the Fickian diffusion and magnetic composite nanoparticles structure disintegration caused by the benzoic-imine bonds dissociating at lower pH, which leading to the shedding of the mPEG layer.

The overall drug release process can be described as: at neutral pH, the complex nanoparticle is relatively stable, the hydrophobic

and π - π stacking interaction between the loaded DOX molecules and benzyl groups restrict the drug release. When the environmental pH is lowered, the intermediate benzoic-imine bonds between PBLA and mPEG start to cleave, the shedding of mPEG layer triggers the quick release of the drug. Meanwhile, the nanoparticles are provided with positively charged surfaces after the shedding of mPEG layer that will be readily taken up by cells.²⁸⁻³⁰

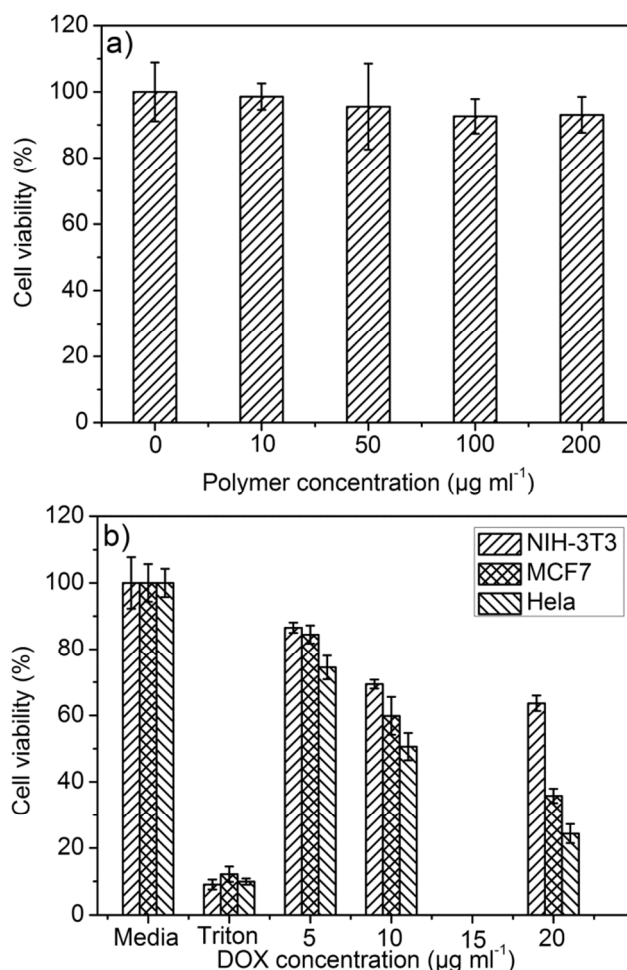


Figure 8. (a) The *in vitro* cytotoxicity studies of FeSi25@PBLA@mPEG on NIH-3T3 cells; and (b) the *in vitro* cytotoxicity studies of FeSi25@PBLA@mPEG@DOX on NIH-3T3, MCF7 and HeLa cells.

An *in vitro* cytotoxicity test (MTT assay) against the NIH/3T3 cells was used to evaluate the biocompatibilities of the magnetic composite nanoparticles, and the corresponding results are revealed in Fig. 8a. The cytotoxicity of the magnetic composite nanoparticles towards NIH/3T3 cells was evaluated after 48 h incubation at concentrations ranging from 10 to 200 $\mu\text{g}\cdot\text{ml}^{-1}$. The cell viability was compared with the control cells that had been incubated in a culture dish without the magnetic composite nanoparticles. The nanoparticles exhibited a good biocompatibility and did not show significant cytotoxicity against NIH/3T3 cells. Fig. 8b shows the cytotoxicity effects of FeSi@PBLA@mPEG@DOX on HIH-3T3, MCF7 and HeLa cells. Cytotoxicity studies reveal that the doxorubicin loaded FeSi@PBLA@mPEG@DOX nanoparticles showed a significant toxicity towards the tested cell lines, compared to normal NIH-

3T3 cells.

Conclusions

A facile method was presented for preparing a magnetic and pH dually responsive multilayer core-shell-corona composite nanoparticle. The shell “grow-from” and “attach-to” approaches were used to produce the polypeptide and mPEG successively coated magnetic/silicone nanoparticles, respectively. The reduction in surface initiator density was achieved by the functionalization/passivation method resulting in a highly polypeptide grafting ratio. The DOX loaded nanoparticles exhibited good super-paramagnetic property and pH-responsible drug release behavior *in vitro*.

Acknowledgments

This work was funded by NSFC (51203079), PCSIRT (IRT1257), NFFTBS (J1103306), and the Ph.D. Programs Foundation for New Teachers of Education Ministry of China (no. 20090031120012).

Notes and references

^a Key Laboratory of Functional Polymer Materials of MOE, Institute of Polymer Chemistry, Nankai University, Tianjin 300071 (PR China). FAX: 86 22 23502749; Tel: +86 22 23507746; E-mail: guolinwu@nankai.edu.cn

^b Collaborative Innovation Center of Chemical Science and Engineering (Tianjin), PR China

† Electronic Supplementary Information (ESI) available: [details of any supplementary information available should be included here]. See DOI: 10.1039/b000000x/

References

- D. Ho, X. Sun and S. Sun, *Accounts of Chemical Research*, 2011, **44**, 875-882.
- D. Yoo, J.-H. Lee, T.-H. Shin and J. Cheon, *Accounts of Chemical Research*, 2011, **44**, 863-874.
- K. J. Widder, A. E. Senyel and G. D. Scarpelli, *Proceedings of the Society for Experimental Biology and Medicine. Society for Experimental Biology and Medicine (New York, N.Y.)*, 1978, **158**, 141-146.
- S. Yu, G. Wu, X. Gu, J. Wang, Y. Wang, H. Gao and J. Ma, *Colloids and Surfaces B-Biointerfaces*, 2013, **103**, 15-22.
- Z. Xu, Y. Feng, X. Liu, M. Guan, C. Zhao and H. Zhang, *Colloids and Surfaces B-Biointerfaces*, 2010, **81**, 503-507.
- T. Verrecchia, G. Spenlehauer, D. V. Bazile, A. Murry-Brelier, Y. Archimbaud and M. Veillard, *Journal of Controlled Release*, 1995, **36**, 49-61.
- M. Ogris, S. Brunner, S. Schuller, R. Kircheis and E. Wagner, *Gene Therapy*, 1999, **6**, 595-605.
- H. Hatakeyama, H. Akita, K. Kogure, M. Oishi, Y. Nagasaki, Y. Kihira, M. Ueno, H. Kobayashi, H. Kikuchi and H. Harashima, *Gene Therapy*, 2007, **14**, 68-77.
- B. Romberg, W. E. Hennink and G. Storm, *Pharmaceutical Research*, 2008, **25**, 55-71.
- Z. Poon, D. Chang, X. Zhao and P. T. Hammond, *ACS Nano*, 2011, **5**, 4284-4292.
- Z. Amoozgar and Y. Yeo, *Wiley Interdisciplinary Reviews: Nanomedicine and Nanobiotechnology*, 2012, **4**, 219-233.
- Y. Yan, G. K. Such, A. P. R. Johnston, H. Lomas and F. Caruso, *ACS Nano*, 2011, **5**, 4252-4257.
- M. Oishi, S. Sasaki, Y. Nagasaki and K. Kataoka, *Biomacromolecules*, 2003, **4**, 1426-1432.
- Y. Bae, N. Nishiyama, S. Fukushima, H. Koyama, M. Yasuhiro and K. Kataoka, *Bioconjugate Chemistry*, 2004, **16**, 122-130.
- A. A. Kale and V. P. Torchilin, *Bioconjugate Chemistry*, 2007, **18**, 363-370.
- N. Murthy, J. Campbell, N. Fausto, A. S. Hoffman and P. S. Stayton, *Bioconjugate Chemistry*, 2003, **14**, 412-419.
- M. Oishi, Y. Nagasaki, K. Itaka, N. Nishiyama and K. Kataoka, *Journal of the American Chemical Society*, 2005, **127**, 1624-1625.
- N. Murthy, J. Campbell, N. Fausto, A. S. Hoffman and P. S. Stayton, *Journal of Controlled Release*, 2003, **89**, 365-374.
- C. Masson, M. Garinot, N. Mignet, B. Wetzter, P. Mailhe, D. Scherman and M. Bessodes, *Journal of Controlled Release*, 2004, **99**, 423-434.
- Y. Chan, V. Bulmus, M. H. Zareie, F. L. Byrne, L. Barner and M. Kavallaris, *Journal of Controlled Release*, 2006, **115**, 197-207.
- S. Lin, F. Du, Y. Wang, S. Ji, D. Liang, L. Yu and Z. Li, *Biomacromolecules*, 2007, **9**, 109-115.
- C. Ding, J. Gu, X. Qu and Z. Yang, *Bioconjugate Chemistry*, 2009, **20**, 1163-1170.
- J. Gu, W.-P. Cheng, J. Liu, S.-Y. Lo, D. Smith, X. Qu and Z. Yang, *Biomacromolecules*, 2007, **9**, 255-262.
- C. Ding, J. Gu, X. Qu and Z. Yang, *Bioconjugate Chemistry*, 2009, **20**, 1163-1170.
- J. H. Jang and H. B. Lim, *Microchemical Journal*, 2010, **94**, 148-158.
- E. Soto Cantu, S. Turksen Selcuk, J. Qiu, Z. Zhou, P. S. Russo and M. C. Henk, *Langmuir*, 2010, **26**, 15604-15613.
- E. Soto-Cantu, R. Cueto, J. Koch and P. S. Russo, *Langmuir*, 2012, **28**, 5562-5569.
- J. Z. Du, T. M. Sun, W. J. Song, J. Wu and J. Wang, *Angewandte Chemie International Edition*, 2010, **49**, 3621-3626.
- Y. Lee, T. Ishii, H. J. Kim, N. Nishiyama, Y. Hayakawa, K. Itaka and K. Kataoka, *Angewandte Chemie International Edition*, 2010, **49**, 2552-2555.
- P. Xu, E. A. Van Kirk, Y. Zhan, W. J. Murdoch, M. Radosz and Y. Shen, *Angewandte Chemie International Edition*, 2007, **46**, 4999-5002.